International Journal of Sustainable Energy Planning and Management

GIS-AHP for Optimal Solar Site Selection: A Case Study of Iraq and Its Implications for Climate Change

Wedyan G. Nassif[a,b]*, Yaseen K. Al-Timimi[b], Dalila Elhmaidi[a]

[a]*Laboratoire de Modélisation Mathématique et de Simulation multi-échelle pour la Physique et l'Ingénieurie (2MSiPI), Faculté des Sciences de Tunis- Université Tunis El Manar, 2092 , Tunis. Tunisia*
[b]*Department of Atmospheric Science, College of Science, Mustansiriyah University, Baghdad, Iraq*

ABSTRACT

Interest in renewable energy sources to meet future energy demands has grown worldwide. This is especially true for wind and solar power, which are emerging sectors that have experienced rapid development in recent years. Large-scale solar photovoltaic (SPV) projects typically take 10–15 years to complete, depending on government approval processes. Factors such as on-site water storage, reliable transportation access, the skills of the local workforce, and the availability of solar panels significantly influence the total project cost. Considering multiple criteria in renewable energy planning is likely to lead to sustainable energy projects.

This study employs Geographic Information Systems (GIS) and Multi-Criteria Decision-Making (MCDM) methods to identify optimal locations for large-scale SPV plants in Iraq. The Analytical Hierarchy Process (AHP) was used to assign weights to each criterion and integrate them into the final suitability map in ArcGIS 10.8. Results indicate that 27,614 km² (6.3% of Iraq's total area) are suitable for SPV installation, with an annual energy potential of 8,700-12,595 MWh per km². If 5–20% of these areas are utilized globally, SPV installations could generate between 3.39 and 13.54 TWh of electricity annually on land, assuming 15% efficiency. Climate models project that average temperatures will reach 34–35°C by 2100, potentially reducing SPV efficiency. This highlights the importance of advanced cooling techniques and heat-resistant materials to prevent long-term performance declines under future climate conditions.

Keywords

Geographic Information System (GIS);
Iraq;
Multi-Criteria Decision-Making (MCDM);
Analytical Hierarchy Process (AHP);
Solar Power

http://doi.org/10.54337/ijsepm.10646

1. Introduction

The global energy landscape is rapidly changing as it moves away from reliance on limited fossil fuels to meet increasing energy demands, driven by greater awareness of the environmental impact of traditional energy sources. Renewable energy has become a central focus worldwide, intersecting with energy security and environmental protection. Among renewable options, solar and wind power are sustainable and abundant, unlike fossil fuels, which are finite and produce greenhouse gases. Rapid technological advances have reduced costs, improved efficiency, and lessened regional conflicts and geopolitical tensions, fostering international cooperation [1,2].

Iraq's economy heavily depends on oil but faces challenges from price volatility and increasing global pressure to transition to a green economy. Its geographic location offers significant potential for developing solar and wind energy, especially in the south and southeast, which could help lower the carbon footprint, enhance energy security, and support economic diversification [3].

Despite this potential, few practical studies have focused on renewable energy adoption in Iraq. Past research has examined hybrid wind-solar systems in select Iraqi cities, highlighting how resource integration can decrease variability throughout the year [4,5]. Although early studies provided initial insights into

*Corresponding author – e-mail: wedyan.atmsc@uomustansiriyah.edu.iq

Received 13.08.2025 | Accepted 13.11.2025 | Published 10.12.2025

List of Nomenclature

GIS	*Geographic Information Systems*
CR	*consistency ratio*
MCDM	*Multi-Criteria Decision-Making*
Hybrid Sites	*Locations suitable for both wind and solar energy generation*
AHP	*Analytical Hierarchy Process*
RI	*Random consistency index*
GHI	*Global Horizontal Irradiance*
SM	*Suitability Maps*
LU	*Land Use*
WOM	*Weight Overlay Model*
SPVP	*Solar Photovoltaic Power Plants*
DEM	*Digital Elevation Model*
SI	*Suitability Index*
CMIP6	*Coupled Model Intercomparison Project Phase 6*

solar radiation modeling and photovoltaic performance, foundational work laid the groundwork for modern solar geometry and irradiance estimation. These pioneering efforts underpin current GIS-based solar mapping and modeling techniques [6,7]. Older studies indicate that Iraq's renewable energy potential remains largely unexploited [8,9].

Comprehensive assessments have also confirmed Iraq's wind energy potential across multiple governorates, emphasizing the country's diverse renewable resources and the need for integrated solar–wind planning strategies, including selecting the most suitable sites for wind energy [10,11]. Projects such as wind-powered street lighting in Dohuk demonstrate the practicality of distributed wind applications in Iraq [12, 13].

Globally, wind energy is expanding rapidly, with installed capacity reaching hundreds of gigawatts [14]. Solar energy has been extensively studied in Iraq, especially in the northern regions, including the use of photovoltaic (PV) systems and thermal storage technologies [15,16]. Recent GIS-AHP applications in Iraq have identified optimal sites for solar farms for example, using GIS-AHP to determine the best locations for solar farms [17], and applying hybrid GIS-Entropy-TOPSIS and AHP-TOPSIS models in Basra for large photovoltaic solar installations [18]. However, these studies are limited either geographically or methodologically, revealing a gap in comprehensive, national-level planning for solar energy in Iraq.

International research indicates that integrating Geographic Information Systems (GIS) with Multi-Criteria Decision-Making (MCDM) tools like the Analytic Hierarchy Process (AHP) offers valuable support for renewable energy planning. Several GIS-based assessments of solar potential in urban areas have considered spatial factors, such as building density and shading, and proposed adaptable methodologies for different regional contexts [19]. Detailed technical and economic analyses have also outlined pathways to achieve 100% renewable energy systems, emphasizing the importance of spatial and system-level planning for large-scale solar integration [20]. Other studies have explored community-level strategies for electricity and storage management in multi-dwelling developments, demonstrating that centralized energy planning can improve efficiency and sustainability in distributed renewable systems [21].

This study aims to conduct a comprehensive national assessment of solar energy potential in Iraq using an integrated GIS–AHP framework. The approach evaluates climatic, geomorphological, economic, infrastructural, and environmental factors to determine optimal sites for photovoltaic (PV) projects. Unlike previous localized or single-method studies, the current work introduces a long-term predictive component by incorporating projected average mean surface air temperature trends until 2100, generated using the Coupled Model Intercomparison Project Phase 6 (CMIP6) dataset under multiple SSP scenarios (SSP1–1.9 to SSP5–8.5).

This integration of spatial decision-making with future climate modeling enables the identification of sites that remain viable under changing climatic conditions. Accordingly, this study provides a novel and comprehensive analytical framework for solar energy planning in Iraq, delivering a long-term spatial decision-support tool for policymakers, investors, and planners to guide sustainable energy transition and enhance national energy resilience

2. Materials and Methods

The goal of this study is to identify the best sites in Iraq for using renewable power sources (solar). This paper primarily employs GIS-MCDM and AHP methods. These tools enable the computational optimization of various geographical, environmental, and technical

factors to determine optimal locations for renewable energy stations as shown in Figure 1.

2.1. Data Collection

In this study, the first step was to identify and gather all essential datasets needed to evaluate solar energy potential. These datasets included global solar radiation to assess the solar resource, land use to identify suitable locations, temperature to determine its effect on energy conversion systems, slope to consider topographic limitations, and distances from power transmission lines, roads, and cities to analyze infrastructure constraints.

Additional climatic and meteorological factors were also incorporated to represent overall site characteristics. Subsequently, the collected data were integrated into a GIS-based Multi-Criteria Decision-Making (MCDM) framework, specifically utilizing the Analytic Hierarchy Process (AHP).

This method enabled a systematic evaluation and weighting of geographical, environmental, and infrastructural parameters to identify the most suitable sites for solar energy development in Iraq. The data were sourced from various references, as shown in Table 1.

Study area

The study area is Iraq, a country with defined international borders, located between 29° 5′ and 37° 22′ N latitudes and 38° 45′ and 48° 45′ W longitudes, covering over 437,049 km² [29]. Figure 2. depicts Iraq's topography.

The terrain varies, featuring plains in the center, marshes in the south, and mountains in the north. Iraq borders six countries: Turkey to the north; Iran to the east; Kuwait and Saudi Arabia to the south; Jordan to the west; and Syria to the northwest. Geographically, Iraq lies in the heart of Western Asia, at the crossroads of three major regions, Anatolia to the north, Persia (Iran) to the east, and the Arabian Peninsula to the south, with the Levant region to the west [30].

The climate is described as continental subtropical, marked by hot, dry summers and cold winters. The central

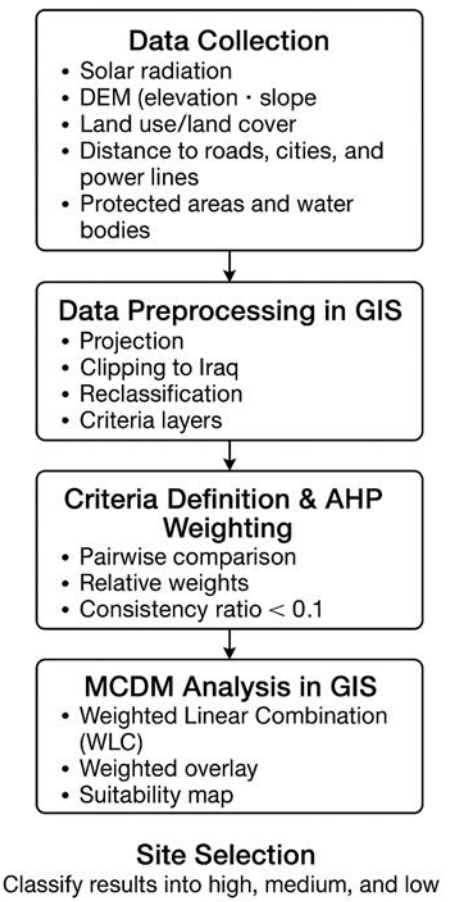

Figure 1: Methodology flowchart for solar site selection in Iraq using GIS-MCDM and AHP.

Table 1: Content of the required data.

No.	Data Source / Organization	Data Type	Data Format	Scale / Resolution	Website / Reference
1	Earth Data / NASA	Solar Radiation / Solar Potential Atlas	Raster Grid (MapInfo-based)	Cell size: 500 m	https://www.earthdata.nasa.gov / [22]
2	National Environmental Authority / Protected Areas Database	National Park Boundaries / Wetland Zones / Protection Zones	ESRI Shape File	1:25,000	Reference [23,24]
3	Agricultural Authority	Agricultural Areas	ESRI Shape File	1:100,000	Reference [25]
4	Iraqi Ministry of Water Resources	Power Lines / Transmission Lines	ESRI Shape / Polyline	Vector data	—
5	Iraqi Ministry of Water Resources	Roads	ESRI Shape / Polyline	Vector data	—
6	Iraqi Ministry of Water Resources	Cities / Settlement Areas	ESRI Shape / Point	Vector data	—
7	Iraqi Ministry of Water Resources	Water Bodies / Boundaries	MapInfo TAB	Vector data	Reference [26]
8	NASA / NOAA	Air Temperature	NetCDF4	—	Reference [27]
9	Derived from DEM (USGS)	Slope	ESRI Grid	Cell size: 100 m	https://earthexplorer.usgs.gov [28]

and southern areas receive little rainfall, whereas the northern region experiences higher precipitation. A broad overview of geopolitics and latitude-longitude data is used for mapping, analysis, and decision-making, especially in GIS-based site selection for renewable energy projects [31,32]. Accurate locational data is vital for practical GIS-MCDM applications, and the findings of this work can be effectively linked to and applied within Iraq's specific geographic and ecological contexts.

3. Statistical analysis

This section presents the statistical methods and analyses employed to evaluate the data collected in the study.

Figure 2: Study Area of Iraq (Source: CIA, 2023)"[33].

Table 2: Satya's Nine-Point Scale of weighting [49].

Value	Semantic meaning
1	These two decision items are equal in weight
3	The decision item that has been selected is weakly more important than the other one.
5	This is the metric that found the selected decision item is much more important than the other one
7	The selected decision item is much more important than the other one
9	The decision item chosen is definitely more critical than the other one
2,4,6,8	Intermediate values

The aim is to provide a clear understanding of the techniques used and the structure of the results presented in the following subsections. This section presents the statistical methods and analyses employed to evaluate the data collected in the study. The aim is to provide a clear understanding of the techniques used and the structure of the results presented in the following subsections.

3.1. Multi-Criteria Decision Analysis and GIS (MCDA-GIS)

Site selection combines Geographic Information Systems (GIS) and Multi-Criteria Decision-Making (MCDM) techniques, especially in renewable energy projects [34]. It integrates GIS and MCDM, allowing the structured evaluation process of MCDM to be combined with the spatial analysis capabilities of GIS.

This method enables the assessment of multiple sites based on various criteria and constraints, using site selection and multi-objective land allocation methods alongside GIS [35].

GIS supports overlay, analysis, and visualization of spatial data to identify suitable locations based on solar radiation and wind speed [36]. The integration of GIS and MCDM helps develop comprehensive topographic and cartographic databases, leading to more reliable, informed decisions in renewable energy site selection [37].

3.2. Weight Overlay Model (WOM)

In GIS, raster data is often categorized into specific ranges, such as slope or Euclidean distance outputs, before being used in the Weighted Overlay tool [38]. Overlay analysis is a powerful technique that combines multiple layers of information, each representing different themes, to thoroughly analyze and reveal their connections [39].

Each range must be assigned a unique value using the Reclassify tool [40]. After reclassification, the point data are incorporated into the weighted overlay process, where an appropriate rating scale is applied.

Raster cells are pre-set to represent indicators such as suitability, preference, risk, or other relevant metrics. Overlay analysis merges features and geometries from different datasets or entities to produce a comprehensive, understandable map [41]. The weighted overlay method captures the core of saliency, using ArcGIS's Weighted Linear Combination (WLC) model as its framework [42]. This GIS-MCDA model usually involves assigning weights to each data layer based on its relative importance. A common approach uses the suitability index (SI), which reclassifies the cell values, as described by Equation 1 [43, 44]:

$$SI = \sum_{i=1}^{n} v_i * w_i \quad (1)$$

i is an indicator, *and* n is the number of indicators. Is the normalized value of indicator i, w_i is the weight of indicator i

3.3. Analytic Hierarchy Process (AHP)

In this study, the AHP method was used to assign appropriate weights or importance levels to the criteria selection. The approach breaks the problem into a hierarchy of overall and sub-criteria through a systematic, dynamic evaluation process [45]. Then, these weights were combined with GIS-MCDM to produce a suitable suitability map [46].

Weights were determined using pairwise comparisons, evaluating each pairing on a scale of 1-9 as shown in table 2 [47] in a standardized manner (for example, one indicates that the criterion in the row has equal importance to the criterion in the column, while a score of 9 indicates that the criterion in the row is significantly more critical than the criterion in the column).

After constructing the pairwise comparison matrix, the weight of each criterion was calculated using Equation 2 [48].

$$F = \begin{bmatrix} x_{11} & x_{12} & x_{13} & \cdots & x_{1n} \\ x_{21} & x_{22} & x_{23} & \cdots & x_{2n} \\ x_{31} & x_{32} & x_{33} & \cdots & x_{3n} \\ \vdots & \vdots & \vdots & \ddots & \vdots \\ x_{m1} & x_{m2} & x_{m3} & \cdots & x_{nn} \end{bmatrix} \quad (2)$$

In (1), the element xij of matrix A(F) of size (n ×n), where i=1, 2, 3⋯n and j=1, 2, 3⋯n, indicates the importance of criterion i.

First, we calculate the total for each column of the pairwise comparison matrix Aij. Next, an entry-wise normalization is performed, dividing each entry by its column sum to obtain a normalized matrix. Since each criterion has a different scale, it is essential to normalize the rating matrix to obtain relative values. The importance of each criterion can then be calculated as the average of the values in each row of the normalized matrix. This average represents a priority vector or the relative significance of the criterion.

The pairwise comparisons must now be checked to ensure logical consistency, thereby increasing confidence in the reliability of the results (Saaty, 1980). CR (Consistency Ratio) is another essential criterion that checks the consistency of the judgments made. CR is derived from the Consistency Index (CI), calculated as shown in equation (3). This is a significant step to verify the appropriateness of the derived weights by calculating the degree of inconsistency in the comparison matrix [50]:

$$CI = \frac{\lambda_{\max} - n}{n-1} \quad (3)$$

Where: $\lambda_{\max}$ is the eigenvalue of the pairwise comparison matrix, and n is the number of criteria.

Finally, the consistency check for the contracted integer value of n is performed using the Consistency Ratio (CR) to evaluate the consistency of the pairwise comparison matrix. Equation 4 [51] gives it:

$$CR = \frac{CI}{RI} \quad (4)$$

RI stands for the Random Consistency Index.

If the Consistency Ratio (CR) is less than or equal to 0.10, the degree of consistency is considered acceptable. However, if CR exceeds 0.10, there are significant inconsistencies in the pairwise comparisons, and the process must be repeated to ensure consistency.

3.4. AHP comparison analysis

The AHP used for SPVP plant site selection has a CR of 4.01%, which is acceptable because it is less than 10%, indicating reliable expert judgment. Although many criteria can significantly influence solar PV site suitability, solar radiation was identified as the most critical factor in Table 3 (relative weight: 39.8%), followed by slope (18.9%) and land use (9.8%).

Location factors related to accessibility, such as distance from roads and power lines, each contributed about 10%. In contrast, the most influential location-based factor, the effect of urban areas, was assigned an 8.9% weight. For the functional suitability analysis, all input layers were reclassified and normalized.

They were then reweighted based on the AHP-derived values and integrated into a GIS environment using the Raster Calculator. The resulting suitability map divided the landscape into four classes, with only contiguous patches larger than 1 km² considered suitable for large-scale solar energy system deployment.

The GIS-MCDM framework for wind and solar energy project site identification in Iraq is illustrated in Figure 3. It involves reclassifying key technical factors, such as solar radiation, and integrating economic factors (slope from DEM), infrastructural factors (distance to roads and grids), and environmental factors (land cover and protected areas).

Climate variables like temperature, precipitation, vegetation index, and soil moisture are also included to support the long-term sustainability of the project. A composite suitability map is then generated by combining these layers through a weighted overlay analysis [52]. Finally, it combines solar assessments, and GRASS GIS-MCDM identifies sites that balance technical, economic, and environmental considerations, demonstrating the effectiveness of GIS-MCDM in meeting the directives of R.H.Q. for renewable energy planning.

3.5. Assessment of Solar Energy Generation

The solar-producing area is determined by excluding unsuitable regions. Then, the technical potential, expressed as the annual solar energy generation capacity at the site, is calculated . The efficiency of solar energy extraction is heavily influenced by the intensity of solar radiation and the performance characteristics of the photovoltaic technology used. The total energy generated at a site depends on solar irradiance, land availability, and the solar energy systems. The potential for

Table 3: Final weights of SPVPS.

Factor	Criteria	Relative Weight Solar PV	Indicator	Suitability
Climatology	GHI (kWh/m^2)	39.8%	<4.2 m/s	Unsuitable
			4.2-5.2	Low Suitable
			5.2-6.2	Moderate Suitable
			>6.2	High Suitable
	Annual Wind Speed (at 50 m)	–	4.7-4.9	Unsuitable
			4.9-5.1	Low Suitable
			5.1-5.4	Moderate Suitable
			5.4-5.6	High Suitable
Topography	Slope degree	18.9%	1-3 %	High Suitable
			3-7	Moderate Suitable
			7-10	Low Suitable
			10-82	Unsuitable
	Land cover/use	9.8%	Water Bodies	Restructure
			Other	Suitable
Availability	Distance from Cities	8.9%	0-2 km	Unsuitable
			2-5	Low Suitable
			5-20	Moderate Suitable
			>20	High Suitable
	Distance from Roads	10%	0-0.5 km	Low Suitable
			0.5-5	High Suitable
			5-20	Moderate Suitable
			>20	Unsuitable
	Distance from the power line	10%	0-0.5 km	Low Suitable
			0.5-5	High Suitable
			5-20	Moderate Suitable
			>20	Unsuitable
	RI	1.32	–	–
		7.412	–	–
	CI	0.063	–	–

annual electrical energy generation is estimated by Equation 5 [53]:

$$E_i = G_i \times A \times A_f \times \eta \times pr \quad (5)$$

E_i is annual electric power generation capacity (GWh/year) and solar yearly radiation received per horizontal unit area (GWh/km2/year). A = Area amount of suitable land available (km^2), for PV installation. Is the area factor: part of the overall making area for a solar panel on suitable land surface. Assumed efficiency of the PV system in converting sunlight into electricity, this is considered to be 10% for this study [54]. The Performance ratio of the PV system, taking into consideration storage and transmission energy losses, with a typical value used in this study equal to 0.75.

System efficiencies differ by technology, with high-efficiency cells usually reaching 36% to 41.1%, while conventional crystalline cells range from 20% to 24%. However, the efficiency used in this study is 14.3%, reflecting the realistic efficiencies seen in existing projects and recommendations from other studies [55].

4. Results

The GIS–AHP spatial analysis offered detailed insights into Iraq's solar energy potential, terrain features, infrastructure access, and the impacts of climate projections. Figures (4–12) and Tables (3–4) present the combined results from spatial data and analytical models.

Figure 4-a shows the spatial distribution of Global Horizontal Irradiance across Iraq, revealing a transparent north–south gradient in solar energy potential. The mountainous Northern provinces have the lowest GHI values, typically below 4.9 kWh/m^2/day, mainly due to higher

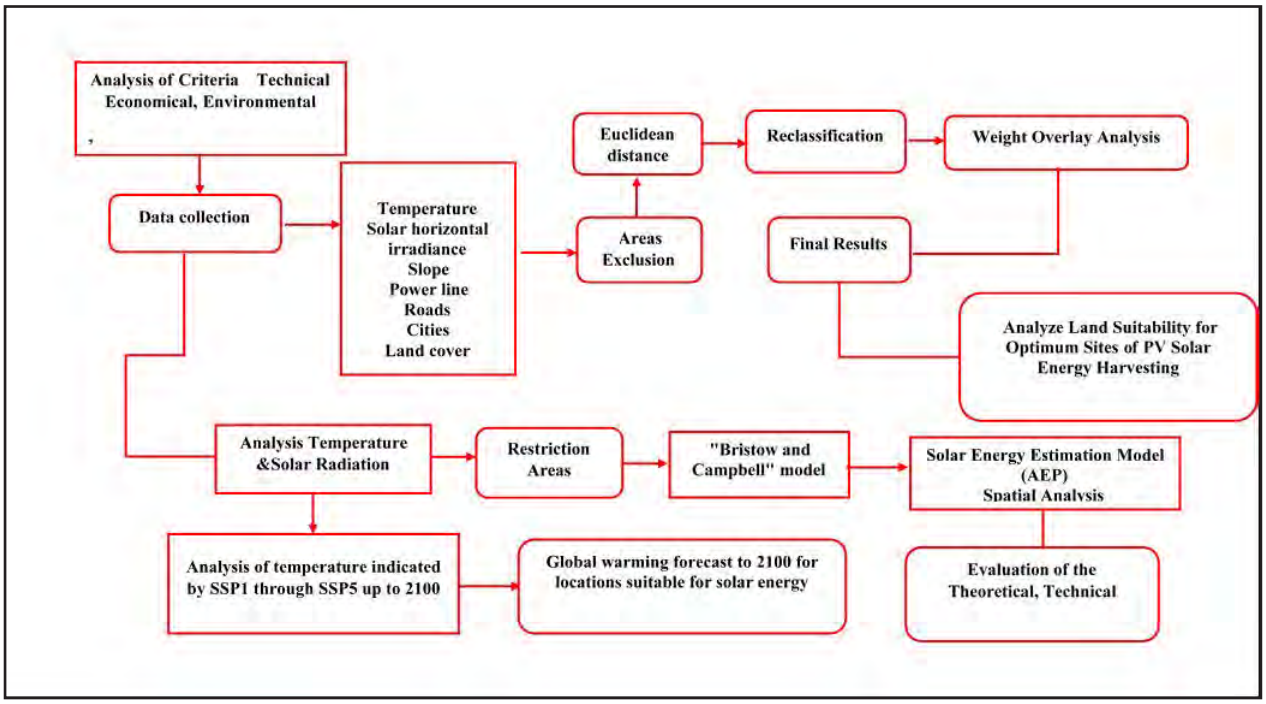

Figure 3: Techniques for Identifying the Most Suitable Sites for Solar Energy.

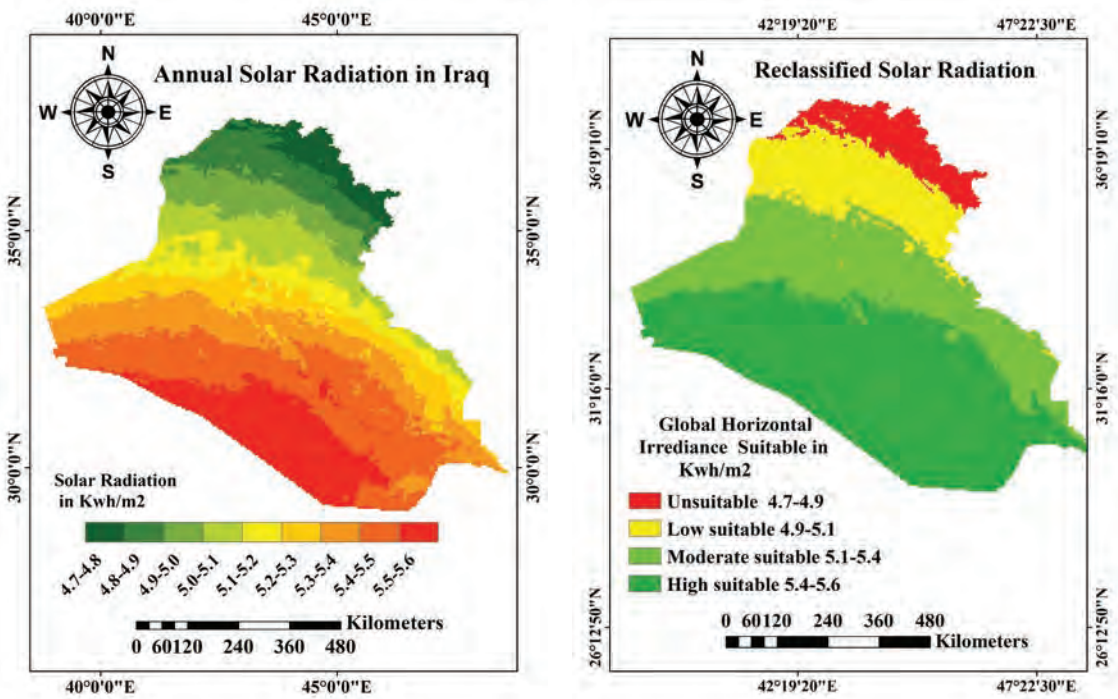

Figure 4:(a) Annual global solar radiation (1980–2022) and (b) solar radiation suitability map of Iraq (Source: *Earth Data/NASA*, Raster Grid, MapInfo-based).

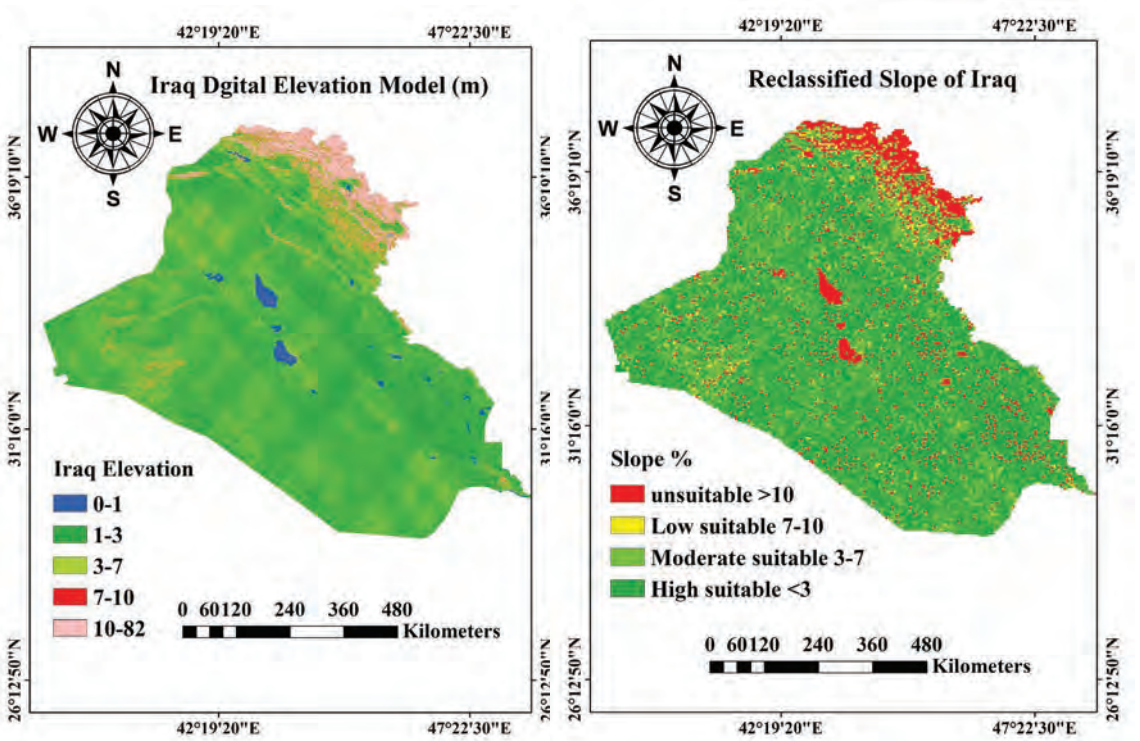

Figure 5: Suitability of Iraq's slope: (a) Elevation after applying the slope tool; (b) Slope reclassification (Source: Derived from DEM, USGS, ESRI Grid).

elevation, persistent cloud cover, and orographic effects. In contrast, the central region experiences moderate irradiance levels ranging from 4.9 to 5.4 kWh/m²/day.

The highest GHI values (5.4–5.6 kWh/m²/ day) are found in the southern governorates (Basra, Maysan, Muthanna, and DhiQar), where low altitude, arid climate, and minimal atmospheric disturbance create ideal conditions for large-scale utility PV and CSP projects. These spatial differences suggest that ground-mounted solar farms should focus on southern areas, while central

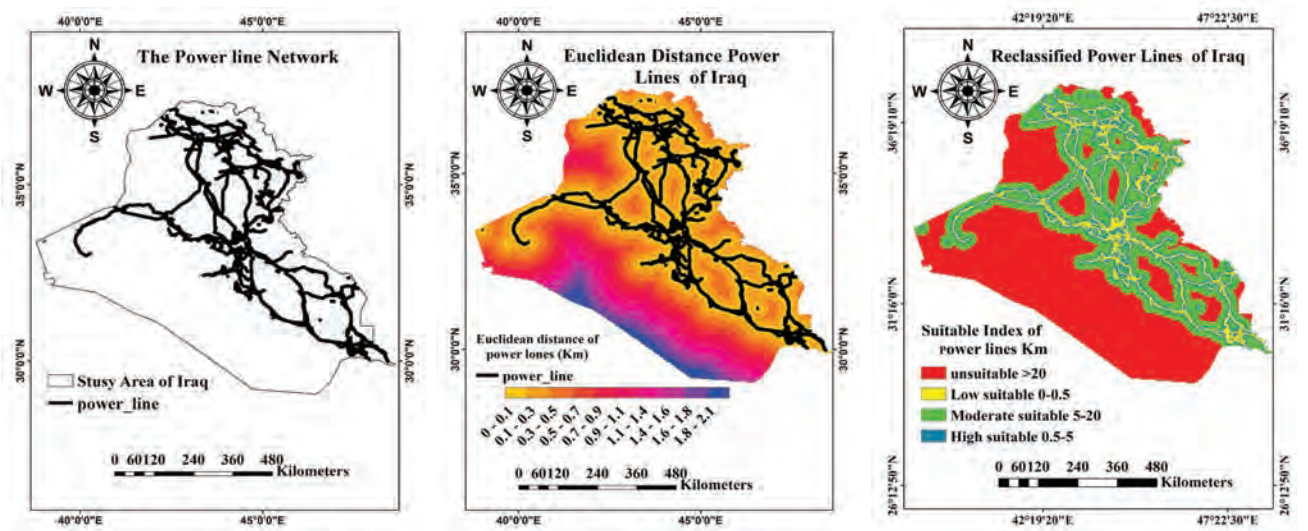

Figure 6: Suitability of distances from power lines in Iraq: (a) Power line network; (b) Euclidean distance from power lines; (c) Reclassified suitability map for grid access (Source: *Iraqi Ministry of Water Resources*, ESRI Shape, Polyline Vector Data).

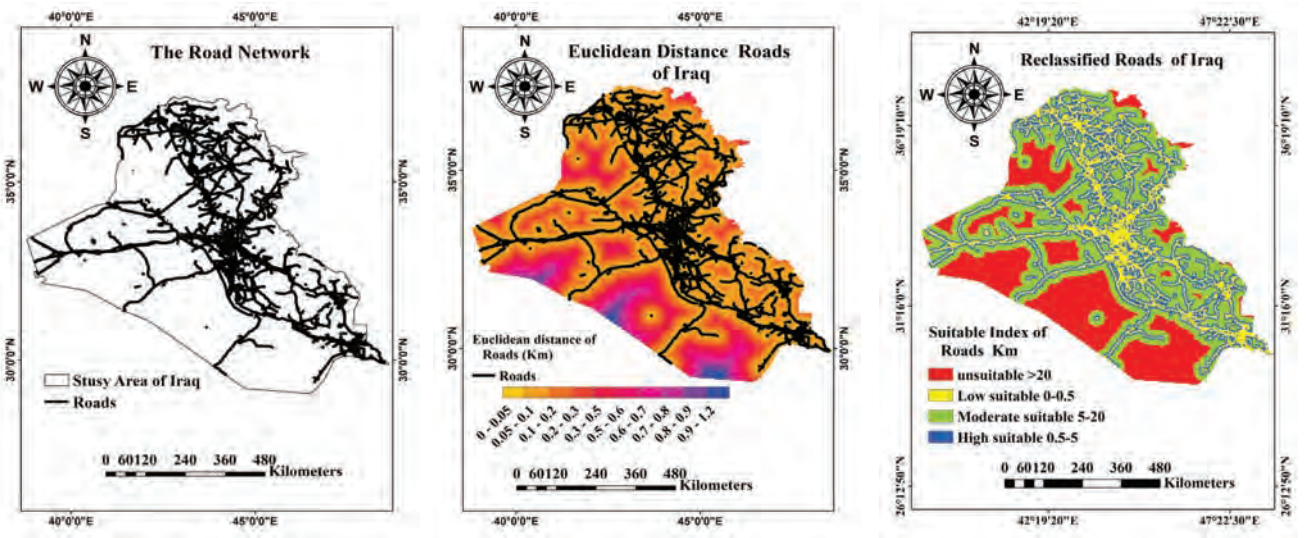

Figure 7: Suitability of distances from roads in Iraq: (a) Road network, (b) Euclidean distance from roads, (c) Reclassified suitability map for roads. (Source: Iraqi Ministry of Water Resources, ESRI Shape/Polyline, Vector data).

regions may be suitable for mid-scale or distributed projects.

The northern highlands are better suited for rooftop or hybrid solutions. Figure 4-b shows the reclassification of raw GHI values into specific suitability categories for solar applications, making them easier to understand by converting continuous irradiance data into practical, operational classes. Areas labeled as "highly suitable" (>5.4 kWh/m²/day) mainly include southern and some southeastern regions; "moderately suitable" zones (4.9–5.4 kWh/m²/day) cover much of the central plains; and "low" and "unsuitable" classes are primarily located in northern highlands and densely urbanized or irrigated areas. This reclassification uses technical thresholds for PV/CSP feasibility and provides a practical layer for shortlisting potential sites where resource quality, land availability, and environmental conditions are favorable.

Figure 5-a shows terrain elevation across Iraq using a high-resolution DEM, highlighting the low-lying Mesopotamian plain in the center and south, and the Zagros-derived uplands in the northeast. Elevation

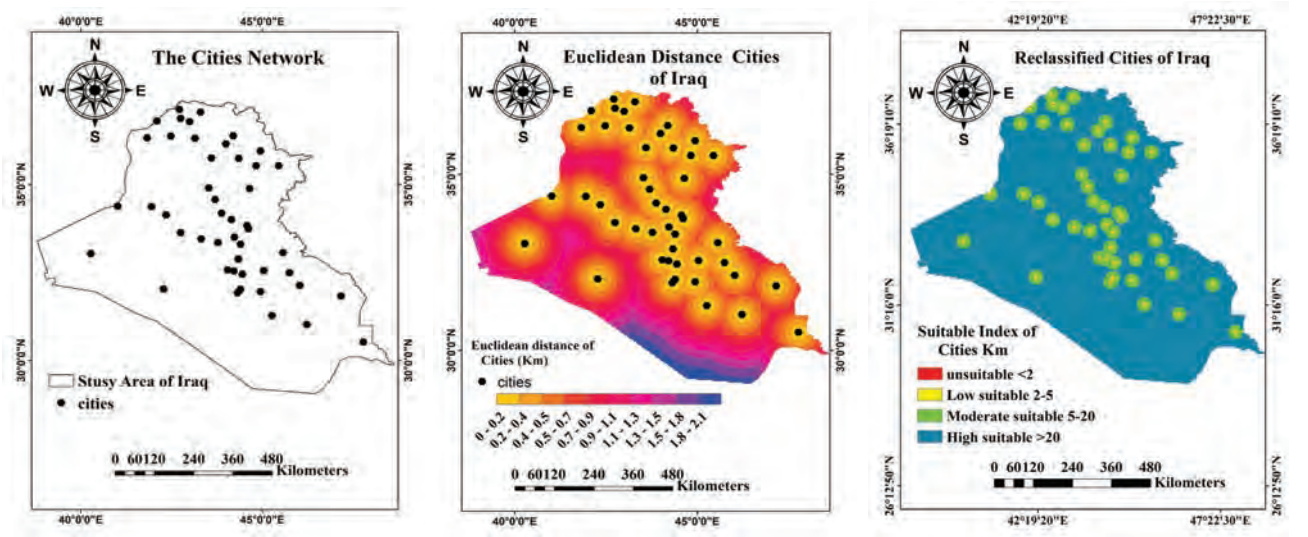

Figure 8: City proximity suitability analysis in Iraq: (a) Distribution of cities, (b) Euclidean distance from cities, (c) Reclassified suitability map. (Source: Iraqi Ministry of Water Resources, ESRI Shape/Point, Vector data).

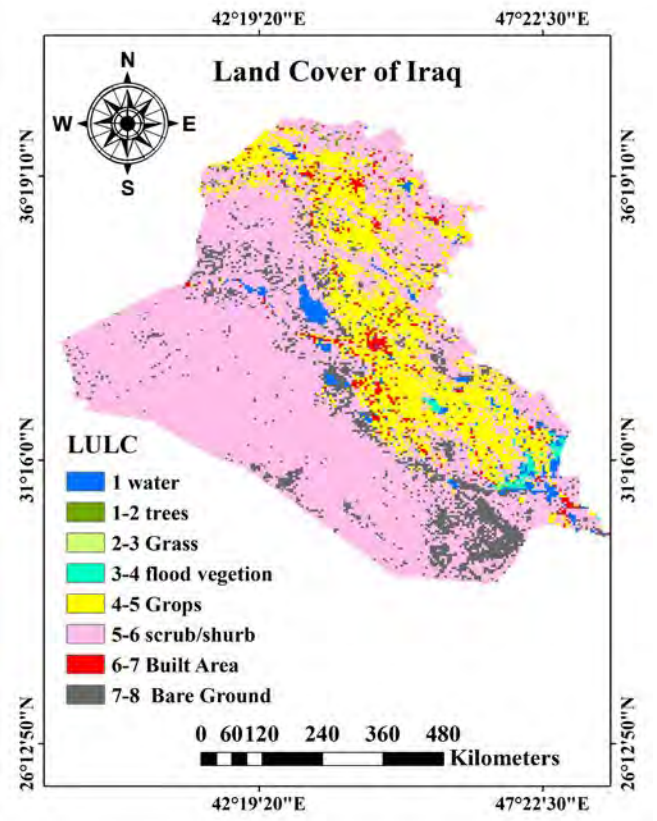

Figure 9: Land Use/Land Cover classification of Iraq. (Source: Global Land Cover by National Mapping Organization, Land Use/ Land Cover, Raster model).

ranges from nearly 0 m in marshes and delta regions to over 82 m in the highlands.

The elevation data helps exclude flood-prone or hydrologically sensitive zones, such as very low-lying marshes, and identify flat areas that can lower civil works and foundation costs for large PV arrays. Therefore, DEM-based elevation is a key factor in suitability modeling, emphasizing the central–southern plains for utility-scale deployment.

Figure 5-b displays slope reclassification into key operational categories (<3%, 3–7%, 7–10%, >10%) and their spatial extent. Most Mesopotamian plain falls within the <3% class, which is highly suitable for ground-mounted PV because it allows for easy racking, reduced earthworks, and minimal shading between rows. Areas with slopes between 3–7% are moderately suitable and may need some grading, while slopes over 7–10% are generally unsuitable for utility-scale PV due to increased construction complexity and costs. This map helps refine site selection by excluding terrain that would significantly raise installation costs or decrease array performance.

Map 5-a helps analyze Iraq's electricity infrastructure and geography. It shows the number of power lines installed and highlights areas needing further development. Combining this map with other data sources can help decision-makers allocate resources more effectively to improve energy access across the country.

Figure 6-b shows the Euclidean distance to the nearest high-voltage transmission line and highlights areas with favorable grid proximity (0.5–5 km). Central and southeastern corridors have dense transmission coverage and short connection distances, which significantly reduce grid interconnection costs and technical challenges for large PV plants. Conversely, western and some northern zones are more than 20 km away, indicating that grid extension or local reinforcement would be needed, increasing project capital costs. Grid proximity is a key economic factor: sites with high irradiance but limited grid access may be deprioritized unless specific network investments are made.

Figure 6-c converts raw distance data into suitability categories for interconnection based on practical thresholds for connection costs and logistics. The reclassified output shows that most high-suitability grid-access cells spatially overlap with high-irradiance and low-slope areas in the south and parts of the central plain, forming a cluster of high-priority zones where technical feasibility and low integration costs are aligned. This integrated grid-access layer balances resource quality with network integration costs.

Table 4: Solar Area Estimates.

Suitability	Estimated Percentage (%)	Available area for Solar Power Plants (km2)
High	6.3%	27,614
Moderate	79.8%	349,985
Low	8.5%	37,257
Unsuitable	5.4%	23,458

The Euclidean distance of roads in Iraq measures the straight-line distance from each site to the nearest road. This metric provides a clear snapshot of nationwide road accessibility. These maps can help us understand the infrastructure and geography of Iraq; they can analyze the spatial distribution and give us an overall view of road coverage and areas that need improvement. Combining these maps with other datasets will enable decision-makers to allocate resources effectively to enhance accessibility and promote equal development across the country, as illustrated in Figure 7-a

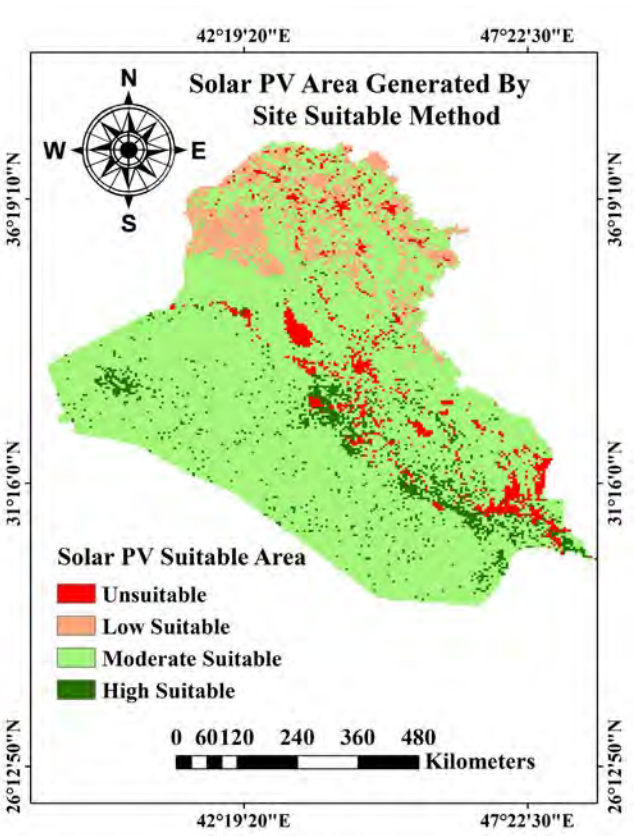

Figure 10: Suitability Map for Solar Photovoltaic Power Plants (SPVPs) in Iraq.

Figure 7-b shows the straight-line distance from each location to the nearest major road, indicating national transport accessibility. Dense road networks in central and southeastern Iraq reduce logistics costs for component delivery, operations, and maintenance access. In contrast, sparse road coverage in the western deserts and the mountainous north increases mobilization costs and complicates construction timelines. Road-distance patterns should be considered early in site screening to avoid selecting resource locations that are economically disadvantaged due to poor transport access.

Figure 7-c reclassifies road proximity into suitability categories, giving the highest scores to sites within a practical haulage distance, such as less than 5 km. When combined with grid proximity and irradiance layers, this map helps identify 'development clusters' where transport logistics, grid access, and solar potential collectively support low-cost, quick deployment.

The Euclidean distances from major cities in Iraq are crucial for planning and developing renewable energy facilities. Being close to urban centers reduces shipping expenses and facilitates the optimal integration of these plants into the energy grid as shown figure 8-a.

Figure 8-b displays the Euclidean distance to major urban centers, highlighting the spatial relationship between generation potential and key demand hubs. Central areas around Baghdad and nearby governorates

Table 5: Estimated Solar Energy Generation and Area Distribution by Region in Iraq.

Region	Coverage (%)	Installed Capacity (MW)	Capacity Factor (CF)	Annual Generation (TWh/year)
South & Southeast	5%	980	0.20	1.715
	10%	1,960	0.20	3.430
	20%	3,920	0.20	6.860
Central & South-Central	5%	760	0.17	1.131
	10%	1,520	0.17	2.262
	20%	3,040	0.17	4.524
North & Northeast	5%	435	0.14	0.539
	10%	870	0.14	1.078
	20%	1,740	0.14	2.156
Total (All Regions)	5%	2,175	—	3.385
	10%	4,350	—	6.770
	20%	8,700	—	13.540

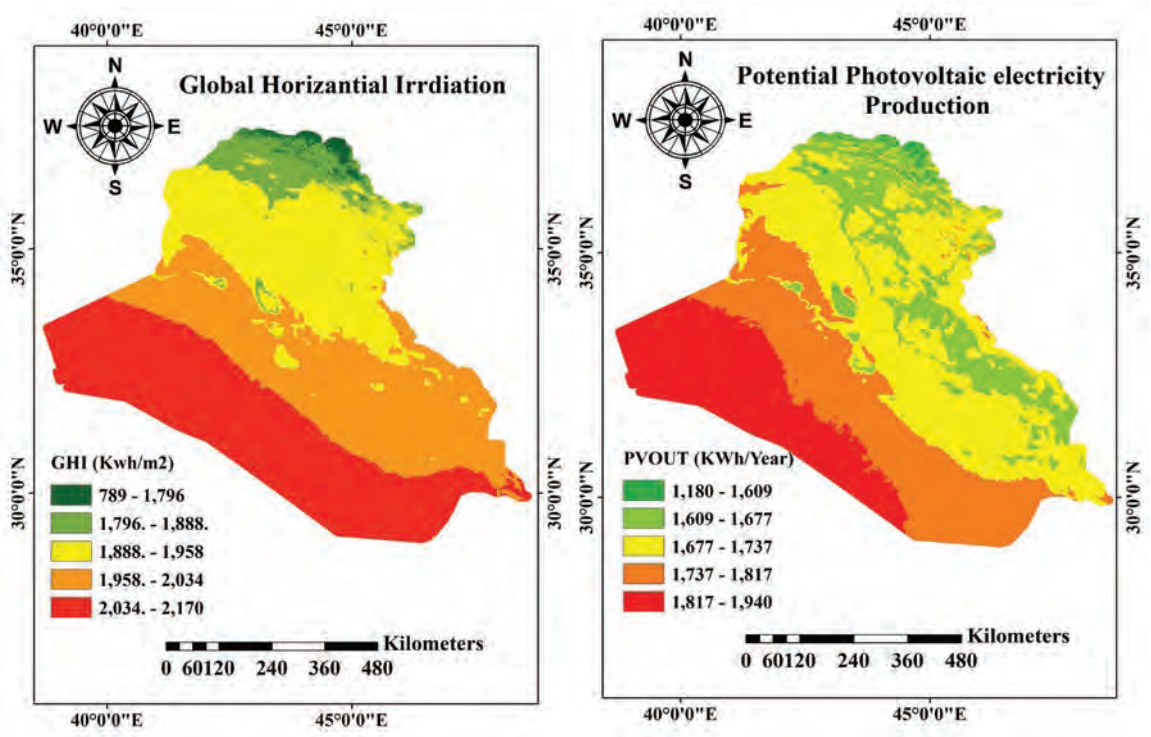

Figure 11. Spatial distribution of solar resources in Iraq: (a) Global Horizontal Irradiance (GHI), (b) Photovoltaic (PV) electricity generation. (Source: Solar Potential Atlas, Raster Grid MapInfo-based).

are close to cities, which supports distributed generation and eases local grid balancing. In contrast, southern production centers are slightly farther from population centers but offer superior resources. Distance-to-demand measures are thus crucial for balancing the trade-offs between maximizing generation (favoring the south) and minimizing transmission losses and distribution costs (favoring central locations).

Figure 8-c classifies peri-urban zones based on combined proximity-to-city and land-availability metrics, identifying fringes where medium-scale PV plants or industrial rooftop installations can be installed with minimal land-use conflicts and strong local demand absorption. This layer supports a strategy that combines utility-scale projects in resource-rich areas with peri-urban generation, aiming to reduce urban demand peaks.

Figure 9 displays a land-cover map that distinguishes water bodies, wetlands, croplands, built-up areas, grassland, and bare ground. Bare and sparsely vegetated surfaces in the south and parts of the west appear as favorable sites due to low ecological sensitivity and minimal vegetation shading, whereas irrigated croplands and wetlands are excluded or marked as low suitability because of concerns about food security and biodiversity. Land cover serves as a key environmental constraint layer in the GIS–AHP model, helping to prevent siting conflicts with sensitive land uses.

Figures 10 show the spatial distribution of solar energy suitability across Iraq by combining various environmental, infrastructural, and climatic factors. The combined GIS–AHP analysis highlights high-suitability zones (about 6.3% of the total area, or 27,614 km²), mainly located in the southern governorates of Basra, Maysan, Najaf, Al-Muthanna, and DhiQar, where flat terrain and high solar irradiance are complemented by accessible infrastructure.

Moderate-suitability areas (79.8% or approximately 349,985 km²) dominate central Iraq (Karbala, Wasit, Diwaniyah, and parts of Anbar and Diyala). These regions could support large-scale solar projects with improvements in transmission and grid capacity.

Low-suitability zones (8.5% or roughly 37,257 km²) and unsuitable regions (5.4% or around 23,458 km²) are mostly situated in the northern highlands (Nineveh, Erbil, Sulaymaniyah, and northern Diyala), where steep slopes, dense vegetation, and urban constraints hinder

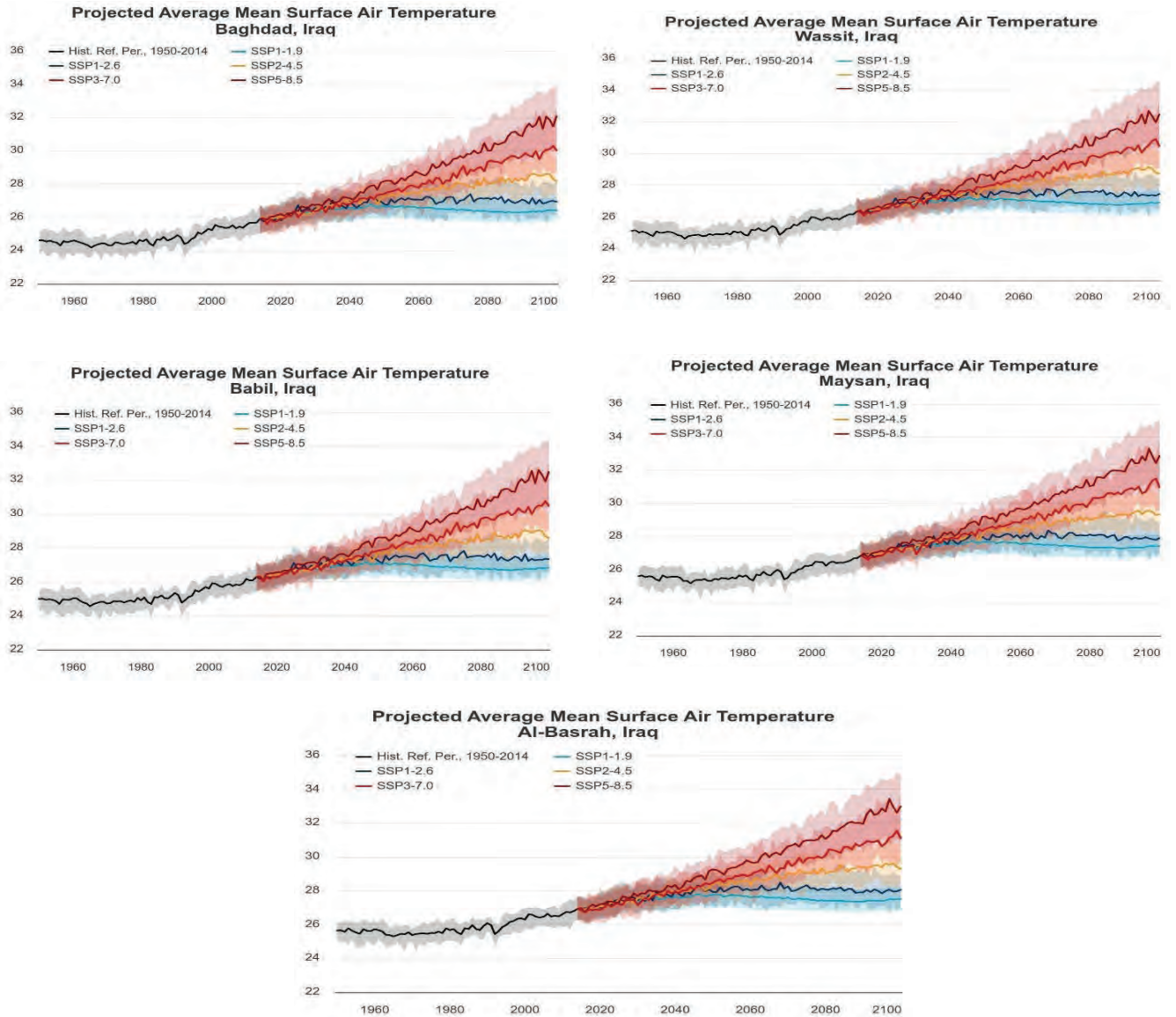

Figure 12. Projected average surface air temperature trends until 2100 for optimal solar energy sites in Iraq, generated using the CMIP6 dataset under different SSP scenarios (SSP1-1.9 to SSP5-8.5). Source: Eyring et al. (2016), CMIP6 Dataset [56, 57].

photovoltaic development. Despite these challenges, these areas may still host hybrid renewable systems (solar–wind or rooftop PV).

Overall, this classification offers a quantitative, spatially detailed basis for decision-makers and investors to focus on southern and central Iraq for immediate development, while designating northern Iraq for future consideration.

Based on the integrated GIS–AHP analysis, four suitability classes were established (Table 4). About 6.3% (27,614 km²) of Iraq is considered highly suitable for solar energy deployment, 79.8% (349,985 km²) is moderately suitable, 8.5% (37,257 km²) is low suitability, and 5.4% (23,458 km²) is unsuitable.The most beneficial areas are the southern provinces (Basra, Muthanna, Maysan, and DhiQar), where solar exposure and terrain work well together.

The study results, shown in Figures (11-a and 11-b), illustrate the spatial distribution of Global Horizontal Irradiance (GHI) and projected annual photovoltaic (PV) energy production in Iraq at a 1 × 1 km² grid resolution. The assessment assumes a performance ratio (PR) of 0.75. It considers 10% of available land as a baseline scenario, with additional scenarios at 5% and

20% land use to estimate technical and realistic solar potential. The results reveal significant regional variation, providing a scientific basis for the systematic deployment of solar energy.

The South and Southeast regions (Basra, Maysan, Al-Muthanna, Najaf, Karbala) display the highest GHI values (1,817–2,170 kWh/m²/year), characterized by flat terrain and long sunshine hours, making them ideal for utility-scale PV installations. With 20% land use, these regions can generate 6.860 TWh/year.

The Central and South-Central areas (Baghdad, Kut, Kirkuk, Diyala, Salah al-Din) experience moderate GHI levels (1,737–2,044 kWh/m²/year), supporting ground-based PV and building-integrated PV (BIPV) systems, with a potential yield of 4.524 TWh/year at 20% land coverage. In contrast, the North and Northeast (Erbil, Mosul, Duhok, Sulaymaniyah) have the lowest GHI (1,180–1,737 kWh/m²/year), mainly due to mountainous terrain and relatively persistent cloud cover. These areas are best suited for decentralized solutions like rooftop PV and microgrids, with an expected output of 2.156 TWh/year.

Table 5 summarizes the estimated installed capacity, capacity factor, and annual generation by region for different land coverage scenarios (5%, 10%, 20%). Increasing land use results in a roughly linear rise in capacity and energy output. The South and Southeast regions dominate the total potential, contributing about 50.7%, followed by central and South Central at 33.4%, and the North and Northeast at 15.9%. At 20% coverage, Iraq's total realistic solar energy potential reaches 13.54 TWh/year, roughly one-third of the current national electricity consumption, highlighting the strategic importance of solar energy as a sustainable and scalable resource. This spatial distribution underscores the need for regionally tailored planning, with utility-scale PV plants in the South, distributed PV systems in central areas, and decentralized rooftop/micro grid solutions in the North. Such an approach offers a practical, bottom-up pathway for developing sustainable solar energy across Iraq.

Figure 12 shows projected average temperature trends for key Iraqi cities under various SSP scenarios (SSP1–1.9 to SSP5–8.5). All scenarios indicate warming throughout the 21st century, with the high-emission SSP5–8.5 forecast suggesting that average annual temperatures in southern cities could rise above 34–35°C by 2100. Elevated ambient temperatures can lower PV conversion efficiency and speed up degradation; therefore, climate projections are included in assessing suitability by highlighting high-temperature areas where technology choices (such as heat-tolerant modules and cooling solutions) and thermal management will be essential to the expected energy outputs.

5. Discussion

The spatial results of this study reveal clear regional differences in Iraq's solar energy potential, with the southern provinces emerging as the most promising due to high irradiance (5.4–5.6 kWh/m²/day) and flat terrain. These findings support previous studies by Khazael & Al-Bakri (2021) and Al-Abadi et al. (2025), which also identified southern Iraq as an ideal location for solar energy investment.

This analysis expands earlier GIS-based assessments by using updated datasets (2025) and incorporating the Analytic Hierarchy Process (AHP) for multi-criteria weighting, providing a comprehensive nationwide framework that considers environmental, technical, and infrastructural factors. The results align with IJSEPM studies (Østergaard et al., 2023; Dvorák et al., 2024), emphasizing the importance of spatial decision-support models for sustainable energy planning. While previous Iraqi studies focused on local assessments, this work offers a full national-scale evaluation of spatial suitability.

The findings highlight Iraq's significant spatial and quantitative solar energy potential and stress the interaction between environmental conditions, infrastructure readiness, and climate change adaptation. The southern and southeastern governorates are the most promising renewable energy corridors due to high irradiance, flat topography, and available land. However, extreme temperatures may reduce PV efficiency, necessitating research into heat-tolerant technologies and effective cooling systems. Topographic and infrastructural analyses demonstrate that accessibility is crucial for economic viability.

Central and south-central regions offer ideal conditions for mid-scale and distributed installations, where integrating with existing grids is most cost-effective. Conversely, the northern highlands, despite lower irradiance and steep terrain, are suitable for hybrid solar–wind projects and decentralized microgrids serving isolated communities. Quantitative analysis (Table 5) shows that utilizing only 20% of suitable land could generate about 13.54 TWh annually, offsetting a significant portion of Iraq's fossil-fuel-based energy consumption. These results support findings by Khazael & Al-Bakri (2021) and Al-Abadi et al. (2025), confirming that solar development in Iraq is both technically feasible and economically viable.

The study also provides a GIS-based framework combining suitability mapping, infrastructure access, and climatic resilience. Climate change implications further emphasize the need for adaptive planning. Under the SSP5–8.5 scenario, rising temperatures, particularly in Basra and Maysan, could affect PV module performance.

Incorporating climate projections into renewable energy planning can safeguard investments through strategies such as reflective PV surfaces, active cooling, and heat-resistant semiconductors. From a policy perspective, a regionally tailored approach is recommended for utility-scale PV plants in the south, distributed generation in the central belt, and hybrid micro grids in the north.

This strategy aligns with Iraq's Nationally Determined Contributions (NDCs) under the Paris Agreement, bolstering energy security, reducing greenhouse gas emissions, and supporting economic diversification. In conclusion, integrating GIS and AHP methods provides a powerful decision-support tool for sustainable energy planning. By combining spatial, infrastructural, and climate data, policymakers can identify optimal solar sites, reduce investment risks, and improve resilience to climate variability.

This framework positions Iraq as a key player in the regional shift toward low-carbon, renewable energy systems, offering long-term environmental and economic benefits.

Conclusion

This study provides a comprehensive national assessment of solar energy potential in Iraq using an integrated GIS–AHP framework. The analysis emphasizes the southern governorates as the most suitable areas for large-scale photovoltaic (PV) deployment due to high solar irradiance, flat terrain, and relatively few land-use restrictions.

The findings validate that Iraq has considerable potential to expand its solar energy capacity, which could significantly assist in diversifying energy sources and lowering greenhouse gas emissions. The GIS–AHP method provides a straightforward, replicable decision-support tool for pinpointing ideal sites and directing renewable energy investments. Future research should incorporate economic feasibility studies, climate resilience modeling, and hybrid decision-making approaches to enhance solar energy planning in Iraq.

Acknowledgements

The authors would like to express their gratitude to the Mustansiriyah University (Baghdad, Iraq) and the Faculty of Sciences at the University of Tunis El Manar (Tunisia) for providing academic and technical support throughout this research. The authors also thank the reviewers and the editorial board of the International Journal of Sustainable Energy Planning and Management for their valuable feedback.

Reference

[1]. Al Garni, H. Z., & Awasthi, A. (2017). Solar PV power plant site selection using a GIS-AHP based approach with application in Saudi Arabia. *Applied energy*, *206*, 1225-1240. https://doi.org/10.1016/j.apenergy.2017.10.024

[2]. Al-Shabeeb, A. R., Al-Adamat, R., & Mashagbah, A. (2016). AHP with GIS for a preliminary site selection of wind turbines in the North West of Jordan. *International Journal of Geosciences*, *7*(10), 1208-1221. http://dx.doi.org/10.4236/ijg.2016.710090

[3]. Hussain, Z. S., Alhayali, S., Dallalbashi, Z. E., Salih, T. K. M., & Yousif, M. K. (2022, July). A look at the wind energy prospects in Iraq. In *2022 International Conference on Engineering & MIS (ICEMIS)* (pp. 1-7). IEEE. https://doi.org/10.1109/ICEMIS56295.2022.9914119

[4]. Dihrab, S. S., & Sopian, K. (2010). Electricity generation of hybrid PV/wind systems in Iraq. *Renewable Energy*, *35*(6), 1303-1307. https://doi.org/10.1016/j.renene.2009.12.010

[5]. Hafez, A. A., Hatata, A. Y., & Aldl, M. M. (2019). Optimal sizing of hybrid renewable energy system via artificial immune system under frequency stability constraints. *Journal of Renewable and Sustainable Energy*, *11*(1). https://doi.org/10.1063/1.5047421

[6]. Liu, B. Y., & Jordan, R. C. (1960). The interrelationship and characteristic distribution of direct, diffuse and total solar radiation. *Solar energy*, *4*(3), 1-19. https://doi.org/10.1016/0038-092X(60)90062-1

[7]. Gueymard, C. A. (2003). Direct solar transmittance and irradiance predictions with broadband models. Part I: detailed theoretical performance assessment. *Solar Energy*, *74*(5), 355-379. https://doi.org/10.1016/S0038-092X(03)00195-6

[8]. Köberle, A. C., Gernaat, D. E., & van Vuuren, D. P. (2015). Assessing current and future techno-economic potential of concentrated solar power and photovoltaic electricity generation. *Energy*, *89*, 739-756. https://doi.org/10.1016/j.energy.2015.05.145

[9]. Obaideen, K., Olabi, A. G., Al Swailmeen, Y., Shehata, N., Abdelkareem, M. A., Alami, A. H., ... & Sayed, E. T. (2023). Solar energy: Applications, trends analysis, bibliometric analysis

and research contribution to sustainable development goals (SDGs). *Sustainability*, *15*(2), 1418. https://doi.org/10.3390/su15021418

[10]. Nassif, W. G., Elhmaidi, D., & Al-Timimi, Y. K. (2024). Selecting Suitable Sites for Wind Energy Harvesting in Iraq using GIS Techniques. *Iraqi Journal of Science*, 5959-5971. https://doi.org/10.24996/ijs.2024.65.10(SI).6

[11]. Mishaal, A. K., Abd Ali, A. M., & Khamees, A. B. (2020, November). Wind distribution map of Iraq-A comparative study. In *IOP Conference Series: Materials Science and Engineering* (Vol. 928, No. 2, p. 022044). IOP Publishing. https://doi.org/10.1088/1757-899X/928/2/022044

[12]. Al-Kayiem, H. H., & Mohammad, S. T. (2019). Potential of renewable energy resources with an emphasis on solar power in Iraq: An outlook. *Resources*, *8*(1), 42. https://doi.org/10.3390/resources8010042

[13]. Abd Ali, L. M., Al-Rufaee, F. M., Kuvshinov, V. V., Krit, B. L., Al-Antaki, A. M., & Morozova, N. V. (2020). Study of hybrid wind–solar systems for the Iraq energy complex. *Applied Solar Energy*, *56*(4), 284-290. https://doi.org/10.3103/S0003701X20040027

[14]. Chaichan, M. T., & Kazem, H. A. (2018). Status of Renewable Energy in Iraq. In *Generating Electricity Using Photovoltaic Solar Plants in Iraq* (pp. 35-45). Cham: Springer International Publishing. https://doi.org/10.1007/978-3-319-75031-6_3

[15]. Al-akayshee, A. S., Kuznetsov, O. N., Alwazah, I., Deeb, M., & Sultan, H. M. (2021, January). Challenges and obstacles facing the growth of using a solar energy in Iraq. In *2021 IEEE Conference of Russian Young Researchers in Electrical and Electronic Engineering (ElConRus)* (pp. 1360-1364). IEEE. https://doi.org/10.1109/ElConRus51938.2021.9396371

[16]. Eroğlu, Ö., Potur, E. A., Kabak, M., & Gencer, C. (2023). A literature review: Wind energy within the scope of MCDM methods. *Gazi University Journal of Science*, *36*(4), 1578-1599. https://doi.org/10.35378/gujs.1090337

[17]. Khazael, S. M., & Al-Bakri, M. (2021). The optimum site selection for solar energy farms using AHP in GIS environment, a case study of Iraq. *Iraqi Journal of Science*, 4571-4587. https://doi.org/10.24996/ijs.2021.62.11(SI).36

[18]. Al-Abadi, A. M., Handhal, A. M., Abdulhasan, M. A., Ali, W. L., Hassan, J. J., & Al Aboodi, A. H. (2025). Optimal siting of large photovoltaic solar farms at Basrah governorate, Southern Iraq using hybrid GIS-based Entropy-TOPSIS and AHP-TOPSIS models. *Renewable Energy*, *241*, 122308. https://doi.org/10.1016/j.renene.2024.122308

[19]. Østergaard, P. A. (2024). Sustainable Energy Planning and Management with PV, Waste heat, positive energy districts and CO2 accounting. *International Journal of Sustainable Energy Planning and Management*, *41*, 1-4. https://doi.org/10.54337/ijsepm.8513

[20]. Connolly, D., & Mathiesen, B. V. (2014). A technical and economic analysis of one potential pathway to a 100% renewable energy system. *International Journal of Sustainable Energy Planning and Management*, *1*, 7-28. https://doi.org/10.5278/ijsepm.2014.1.2

[21]. Tomc, E., & Vassallo, A. M. (2018). Community electricity and storage central management for multi-dwelling developments: an analysis of operating options. *International Journal of Sustainable Energy Planning and Management*, *17*, 15-30. https://doi.org/10.5278/ijsepm.2018.17.3

[22]. Hussain, M. T., & Mahdi, E. J. (2018, May). Assessment of solar photovoltaic potential in Iraq. In *Journal of Physics: Conference Series* (Vol. 1032, No. 1, p. 012007). IOP Publishing. https://doi.org/10.1088/1742-6596/1032/1/012007

[23]. Stevens, M. L. (2007). Iraq and Iran in ecological perspective: the Mesopotamian marshes and the Hawizeh-Azim Peace Park. *Peace Parks: Conservation and Con ict Resolution*, 313-32.https://books.google.tn/books/content?id=pae0qMYFtaUC&pg=PA376&img=1&zoom=3&hl=en&sig=ACfU3U2qYcRrzK7xz5zirwsMVQrlBogsaw&w=1280

[24]. Alabbas, A. A. K., & Alumery, A. O. A. (2022). Comparative Study of Environmental Protected Areas Laws and Legislation Between Iraqi and Its Neighbors. *International Journal of Sustainable Development & Planning*, *17*(7). https://doi.org/10.18280/ijsdp.170705

[25]. Al-Ansari, N., Abed, S. A., & Ewaid, S. H. (2021). Agriculture in Iraq. *Journal of Earth Sciences and Geotechnical Engineering*, *11*(2), 223-241. https://doi.org/10.47260/jesge/1126

[26]. Erzaij, K. R., Hatem, W. A., & Maula, B. H. (2020). Applying intelligent portfolio management to the evaluation of stalled construction projects. *Open Engineering*, *10*(1), 552-562. https://doi.org/10.1515/eng-2020-0064

[27]. Understanding Weighted Overlay," ESRI, 2014. [Online]. Available: https://www.esri.com/about/newsroom/arcuser/understanding-weighted-overlay/

[29]. Jasim, A. I., & Awchi, T. A. (2020). Regional meteorological drought assessment in Iraq. *Arabian Journal of Geosciences*, *13*(7), 284. https://doi.org/10.1007/s12517-020-5234-y

[30]. Al-Timimi, Y. K., & Al-Khudhairy, A. A. (2018, May). Spatial and Temporal Temperature trends on Iraq during 1980-2015. In *Journal of Physics: Conference Series* (Vol. 1003, No. 1, p. 012091). IOP Publishing. https://doi.org/10.1088/1742-6596/1003/1/012091

[31]. Al-Salihi, A. M., & AL-Ramahy, Z. A. (2017). A neural network model for estimation soil temperature bases on limited meteorological parameters in selected provinces in Iraq.

Journal of Applied and Advanced Research, *2*(5), 292-300. http://dx.doi.org/10.21839/jaar.2017.v2i5.106

[32]. Abass, A. Z., & Pavlyuchenko, D. A. (2019). The exploitation of western and southern deserts in Iraq for the production of solar energy. *International Journal of Electrical and Computer Engineering*, *9*(6), 4617. https://doi.org/10.11591/ijece.v9i6.pp4617-4624

[33]. CIA. (2023). *Iraq — Political Map*. The World Factbook. Central Intelligence Agency. Available at: https://www.cia.gov/the-world-factbook/countries/iraq/

[34]. Wang, Y., Tao, S., Chen, X., Huang, F., Xu, X., Liu, X., ... & Liu, L. (2022). Method multi-criteria decision-making method for site selection analysis and evaluation of urban integrated energy stations based on geographic information system. *Renewable energy*, *194*, 273-292. https://doi.org/10.1016/j.renene.2022.05.087

[35]. Villacreses, G., Jijón, D., Nicolalde, J. F., Martínez-Gómez, J., & Betancourt, F. (2022). Multicriteria decision analysis of suitable location for wind and photovoltaic power plants on the Galápagos Islands. *Energies*, *16*(1), 29. https://doi.org/10.3390/en16010029

[36]. Xu, Y., Li, Y., Zheng, L., Cui, L., Li, S., Li, W., & Cai, Y. (2020). Site selection of wind farms using GIS and multi-criteria decision making method in Wafangdian, China. *Energy*, *207*, 118222. https://doi.org/10.1016/j.energy.2020.118222

[37]. Ali, S., Taweekun, J., Techato, K., Waewsak, J., & Gyawali, S. (2019). GIS based site suitability assessment for wind and solar farms in Songkhla, Thailand. *Renewable Energy*, *132*, 1360-1372.. https://doi.org/10.1016/j.renene.2018.09.035

[38]. Malczewski, J., & Rinner, C. (2015). *Multicriteria decision analysis in geographic information science* (Vol. 1, pp. 55-77). New York: Springer. https://link.springer.com/book/10.1007/978-3-540-74757-4

[39]. Stanzione, T., & Lashlee, J. D. (2008). *Geospatially enabled modeling and simulation*. Society for Modeling & Simulation International. https://proceedings.esri.com/library/userconf/feduc08/papers/gems_feduc2008.pdf

[40]. de Lange, N. (2023). *Geoinformatics in Theory and Practice*. https://link.springer.com/book/10.1007/978-3-662-65758-4

[41]. Danielson, M., & Ekenberg, L. (2017). A robustness study of state-of-the-art surrogate weights for MCDM. *Group Decision and Negotiation*, *26*(4), 677-691.https://doi.org/10.1007/s10726-016-9494-6

[42]. Polo-Castañeda, M., Gomez-Rojas, J., & Linero-Cueto, J. (2021). Application of AHP and GIS for determination of suitable wireless sensor network zones for oceanographic monitoring in the South Caribbean Sea upwelling zone. *Int. J. Adv. Sci. Eng. Inf. Technol*, *11*(5), 1696-1703. https://doi.org/10.18517/ijaseit.11.5.14293

[43]. Danielson, M., & Ekenberg, L. (2017). A robustness study of state-of-the-art surrogate weights for MCDM. *Group Decision and Negotiation*, *26*(4), 677-691. https://doi.org/10.1007/s10726-016-9494-6

[44]. Saraswat, S. K., Digalwar, A. K., Yadav, S. S., & Kumar, G. (2021). MCDM and GIS based modelling technique for assessment of solar and wind farm locations in India. *Renewable Energy*, *169*, 865-884.https://doi.org/10.1016/j.renene.2021.01.056

[45]. Gacu, J. G., Garcia, J. D., Fetalvero, E. G., Catajay-Mani, M. P., & Monjardin, C. E. F. (2023). Suitability analysis using GIS-based analytic hierarchy process (AHP) for solar power exploration. *Energies*, *16*(18), 6724. https://doi.org/10.3390/en16186724

[46]. Xie, J., Zhang, H., Wang, Z., & Guo, X. (2022, May). Research on multi-target selection and sequencing based on analytic hierarchy process. In *Journal of Physics: Conference Series* (Vol. 2221, No. 1, p. 012044). IOP Publishing. https://doi.org/10.1088/1742-6596/2221/1/012044

[47]. Liang, F., Brunelli, M., & Rezaei, J. (2020). Consistency issues in the best worst method: Measurements and thresholds. *Omega*, *96*, 102175. https://doi.org/10.1016/j.omega.2019.102175

[48]. Stofkova, J., Krejnus, M., Stofkova, K. R., Malega, P., & Binasova, V. (2022). Use of the analytic hierarchy process and selected methods in the managerial decision-making process in the context of sustainable development. *Sustainability*, *14*(18), 11546. https://doi.org/10.3390/su141811546

[49]. Zhang, Z., Liu, X., & Yang, S. (2009, June). A note on the 1–9 scale and index scale in AHP. In *International Conference on Multiple Criteria Decision Making* (pp. 630–634). Berlin, Heidelberg: Springer. https://doi.org/10.1007/978-3-642-02279-1_91

[50]. Rezaei, J. (2015). Best-worst multi-criteria decision-making method. *Omega*, *53*, 49-57 https://doi.org/10.1016/j.omega.2014.11.009

[51]. Rahimi, I., Azeez, S. N., & Ahmed, I. H. (2019). Mapping forest-fire potentiality using remote sensing and GIS, case study: Kurdistan Region-Iraq. In *Environmental remote sensing and GIS in Iraq* (pp. 499-513). Cham: Springer International Publishing. https://doi.org/10.1007/978-3-030-21344-2_20

[52]. Zhang, Y., Ren, J., Pu, Y., & Wang, P. (2020). Solar energy potential assessment: A framework to integrate geographic, technological, and economic indices for a potential analysis. *Renewable Energy*, *149*, 577-586.https://doi.org/10.1016/j.renene.2019.12.071

[53]. Sedrati, M., Maanan, M., & Rhinane, H. (2019). PV power plants sites selection using gis-fahp based approach in north-western morocco. *The International Archives of the Photogrammetry, Remote Sensing and Spatial Information Sciences*, *42*, 385-392.https://doi.org/10.5194/isprs-archives-XLII-4-W19-385-2019

[54]. Asakereh, A., Soleymani, M., & Sheikhdavoodi, M. J. (2017). A GIS-based Fuzzy-AHP method for the evaluation of solar farms locations: Case study in Khuzestan province, Iran. *Solar Energy*, *155*, 342-353.https://doi.org/10.1016/j.solener.2017.05.075

[55]. Shen, H., Walter, D., Wu, Y., Fong, K. C., Jacobs, D. A., Duong, T., ... & Catchpole, K. R. (2020). Monolithic perovskite/Si tandem solar cells: pathways to over 30% efficiency. *Advanced energy materials*, *10*(13), 1902840. https://doi.org/10.1002/aenm.201902840

[56]. Eyring, V., Bony, S., Meehl, G. A., Senior, C. A., Stevens, B., Stouffer, R. J., & Taylor, K. E. (2016). Overview of the Coupled Model Intercomparison Project Phase 6 (CMIP6) experimental design and organization. *Geoscientific Model Development*, *9*(5), 1937-1958. https://doi.org/10.5194/gmd-9-1937-2016

[57]. World Climate Research Programme (WCRP)**.** *Coupled Model Intercomparison Project Phase 6 (CMIP6) – Official Dataset Portal*. Available online: https://wcrp-cmip.org/cmip6/